Electric Unicycle from Image Signals

[1]Yuan-Pao Hsu, [2]Sheng-Han Huang, [3]Chien-Hung Kuo, [4]Hung-Chih Chen
Dept. of Computer Science and Information Engineering
National Formosa University
Yunlin, Taiwan
[1]hsuyp@nfu.edu.tw, [2]tom.s-0126@yahoo.com.tw, [3]jonnydy@hotmail.com, [4]houmze@gmail.com

Abstract — This paper realizes a SoPC system which balances an electric unicycle based on image data from a CMOS camera. Generally, tilt-meters and gyros have commonly been chosen to measure the tilt angle and angle rate of a unicycle. In this paper, a CMOS camera is employed as the tilt angle measurement sensor instead. Through simple image processing techniques, a hardware circuit module for inclination measurement for the unicycle is implemented on the FPGA of a SoPC. By the concept of software hardware co-design, the inclination measurement module is integrated with the double-PD control method on the SoPC to balance the unicycle. Simulation and experimental results confirm that the resulting system meets the design goal.

Keywords — SoPC, FPGA, electric unicycle, double-PD control

I. INTRODUCTION

In order to get rid of petroleum dependency and cost down, the industry and academy have spent lots of efforts on researching and developing electric wheeled vehicles. Among which, electric self-balancing vehicles have also drawn much attention and some products even can be found off the shelf, for instance, RYNO Motor, Segway, and UNO III [1-3]. The main advantage of an electric self-balancing vehicle is that it can keep balancing while moving. Besides, the turning radius and the size of the vehicle are quite small. For achieving these advantages, an accurate and reliable controller is required.

An electric unicycle is a non-linear and unstable system such that, from the viewpoint of control, it has been a challenging system to be well controlled. Ruan et al derived the dynamic model of a unicycle robot, which composed of a wheel, a frame and a disk, by using Euler-Lagrange method [4]. Under state space control method, the unicycle can reach longitudinal stability by appropriate control to the wheel and lateral stability by adjusting appropriate torque imposed by the disk. Jin and Zhang designed a path planning algorithm to control a unicycle according to the POS (Particle Swarm Optimization) method [5]. Lee designed and implemented a PID controller to control an electric unicycle [6]. Chen derived a unicycle mathematical model and designed feedback linearization and sliding mode control methods to verify a real-time hardware-in-the-loop (HIL) platform [7]. Huang designed and realized an unmanned electric unicycle system controlled by pole-placement and LQR (Linear-Quadric Regulator) methods [8]. Tsai et al developed an electric unicycle, which can be ridden by one person, under the control of an adaptive nonlinear control method [9].

The electric unicycle has often used tilt-meters and gyros to measure its angle of inclination and angle rate. In this paper, however, a CMOS camera is employed as the measurement sensor. The function of the camera captures images and there is a reference horizontal line in each image. According to the line in the image the unicycle's body tilt angle can be computed. Adopting the image processing procedure like the method used in [10], the image processing unit will be designed as a hardware circuit module and implemented inside the FPGA (Field Programmable Gate Array) of a SoPC (System on a Programmable Chip). By the concept of software and hardware co-design, the inclination measurement module will be integrated with a double-PD controller to be realized on the SoPC to balance the unicycle.

The organization of this article is as follows. Mathematical model of the unicycle is derived in Section II. Section III describes the PD control method briefly. Simulation results are demonstrated in Section IV. System architecture of the unicycle is elucidated in Section V, whereas Section VI explains the design of the image processing unit. Section VII shows experiment results. Finally, conclusions and future perspective are drawn.

II. MATHEMATICAL MODEL DERIVATION OF A UNICYCLE

Figure 1 depicts the basic architecture with parameters of a unicycle. The relative parameters are defined in Table 1.

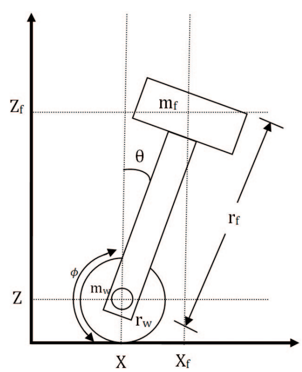

Figure 1. Unicycle architecture

TABLE I.
DEFINITION OF RELATIVE PARAMETERS OF THE UNICYCLE

Symbol	Definition	Unit
θ	Inclination angle of the body	rad
ϕ	Wheel rotation angle	rad
m_f	Mass of the body	kg
m_w	Mass of the wheel	kg
r_f	Length between the wheel axle and center of mass of the body	m
r_w	Radius of the wheel	m
x_f	Distance between center of mass of the body and z axis	m
z_f	Distance between center of mass of the body and x axis	m
x	Distance between the wheel axle and z axis	m
z	Distance between the wheel axle and x axis	m
μ_ϕ	Coefficient of viscous friction between the wheel and ground	Nm•sec/rad
g	Gravitational acceleration	m/sec^2
Im	Moment of inertia of the motor axle	Kgm^2
dl	Reduction ratio of gear	

Euler-Lagrange equations of the unicycle can be written as (1).

$$\begin{cases} \dfrac{d}{dt}\left(\dfrac{\partial L}{\partial \dot{\phi}}\right) - \dfrac{\partial L}{\partial \phi} = -\mu_\phi \dot{\phi} + \tau \\ \dfrac{d}{dt}\left(\dfrac{\partial L}{\partial \dot{\theta}}\right) - \dfrac{\partial L}{\partial \theta} = 0 \end{cases} \tag{1}$$

Where Lagrangian function L is defined in (2).

$$L = T - U \tag{2}$$

T and U are kinetic and potential energy, respectively, and are shown in (3) and (4).

$$\begin{aligned} T =& \left(\frac{1}{2}m_w r_w^2 + \frac{1}{2}m_f r_w^2\right)\dot{\phi}^2 + r_w r_f \dot{\phi}\dot{\theta}\cos\theta + \frac{1}{2}m_f r_f^2 \dot{\theta}^2 \\ &+ \frac{1}{2}I_w \dot{\phi}^2 + \frac{1}{2}I_f \dot{\theta}^2 + \frac{1}{2}I_m dl^2 \left(\dot{\phi} - \dot{\theta}\right)^2 \end{aligned} \tag{3}$$

$$U = m_w g r_w + m_f g (r_w + r_f \cos\theta) \tag{4}$$

Substituting (2), (3), and (4) into (1), we have mathematical model of the unicycle as demonstrated in (5).

$$\begin{cases} \ddot{\phi} = \dfrac{b_2}{b_1}\dot{\theta}^2 + \dfrac{b_3}{b_1} + \dfrac{b_4}{b_1}\dot{\phi} + \dfrac{1}{b_1}\tau \\ \ddot{\theta} = \dfrac{c_1 b_2}{b_1}\dot{\theta}^2 + \dfrac{c_1 b_3}{b_1} + \dfrac{c_1 b_4}{b_1}\dot{\phi} + \dfrac{c_1}{b_1}\tau + \dfrac{1}{2a_2} m_f g r_f \sin\theta \end{cases} \tag{5}$$

Where

$$a_1 = \frac{1}{2}m_w r_w^2 + \frac{1}{2}m_f r_w^2 + \frac{1}{2}I_w + \frac{1}{2}I_m dl^2 \tag{6}$$

$$a_2 = \frac{1}{2}m_f r_f^2 + \frac{1}{2}I_f + \frac{1}{2}I_m dl^2 \tag{7}$$

$$b_1 = 2a_1 - \frac{1}{2a_2}\left(m_f r_w r_f \cos\theta - I_m dl^2\right)^2 \tag{8}$$

$$b_2 = m_f r_w r_f \sin\theta \tag{9}$$

$$b_3 = -\frac{1}{2a_2} m_f g r_f \sin\theta\left(m_f r_w r_f \cos\theta - I_m dl^2\right) \tag{10}$$

$$b_4 = -\mu_\phi \tag{11}$$

$$c_1 = -\frac{1}{2a_2}\left(m_f r_w r_f \cos\theta - I_m dl^2\right) \tag{12}$$

III. PD CONTROL

A PD controller consists of proportional control and derivative control, as demonstrated in Figure 2. The designer adjusts proportional gain K_p and derivative gain K_d in order that the controller can output appropriate control value u(t) to minimize the error e(t) for achieving expected control performance. The relationship between input and output of a PD controller is as equation (13) shows.

$$u(t) = k_p \cdot e(t) + k_d \cdot \frac{d}{dt}e(t) \tag{13}$$

The PD controller is a SISO (single-input single-output) system. If we want to balance the unicycle and keep the displacement of the unicycle not far away from a certain starting location at the same time, it requires a system composed of two PD controllers, one for controlling the inclination, θ, and another for the wheel angle, ϕ. The structure of the double-PD controller is shown in Figure 3 in which the output of each PD controller is summed up to be the control value, u, in each control step.

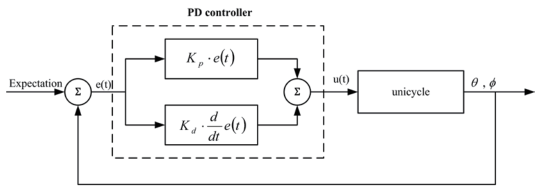

Figure 2. Structure of a PD controller

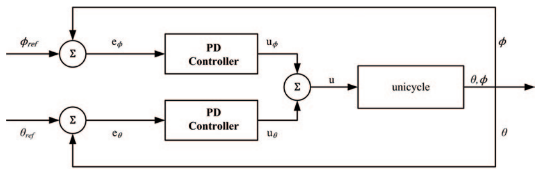

Figure 3. Structure of a double-PD controller

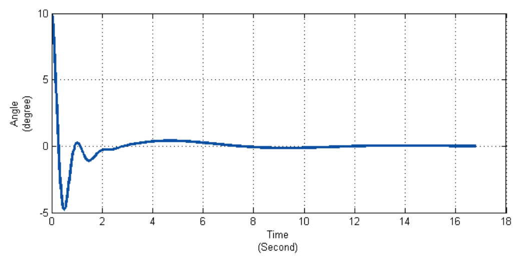

Figure 4. Unicycle inclination variances under double-PD control

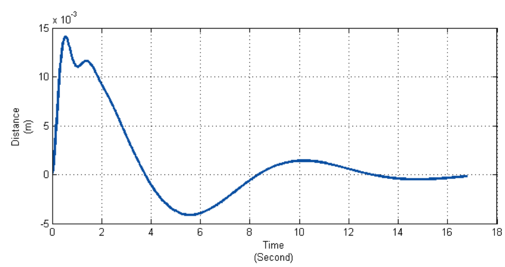

Figure 5. Unicycle displacement variances under double-PD control

TABLE II.
PARAMETERS OF THE UNICYCLE IN SIMULATION

Symbol	Definition	Value
m_f	Mass of the body	11(kg)
I_f	Moment of inertial of the body	2.3467(kg)
r_f	Length between the wheel axle and center of mass of the body	0.8(m)
r_w	Radius of the wheel	0.075(m)
m_w	Mass of the wheel	1(kg)
I_w	Moment of inertial of the wheel	0.5625(m)
μ_ϕ	Coefficient of viscous friction between the wheel and ground	0.001(Nm•sec/m)
g	Gravitational acceleration	9.81(m/sec^2)
I_m	Moment of inertia of the motor axle	0.611x10-4(Kg•m^2)
d_l	Reduction ratio of gear	30

IV. SIMULATION RESULTS

Figure 4 and 5 are simulation results of the unicycle, with initial inclination 10° and other parameters listed in Table 2, under the control of the double-PD control method by choosing $K_{p\theta} = 80$, $K_{d\theta} = 10$, $K_{p\phi} = 0.2$, and $K_{d\phi} = 0.2$. After about 2.9 seconds, the unicycle reached stabilization at round 0 degree of inclination and ±0.5 cm of displacement.

V. SYSTEM ARCHITECTURE

Demonstrated in Figure 6 is the system architecture of the implemented electric unicycle. The operation process of the system starts from that the CMOS image sensor captures an image and sends the image to the image processing circuit and the motor encoder sends pulses to the pulse counting circuit for computing motor speed as well. The image processing result and motor speed are transferred to the balancing controller to calculate the control value. Finally, the D/A converter converts the control value into analog voltage for motor driver module to drive the motor.

Figure 7 is the partition of the FPGA, where the image processing unit and motor speed counter are implemented by hardware, and the rest of the system is implemented in software which is responsible by the Nios II processor. The software and hardware are combined by the design methodology of software/hardware co-design.

Figure 8 shows the resulting structure of the system consisting of a DC servo motor, a COMS camera, a SoPC, a motor driver, a D/A converter, a wheel, and the skeleton with 80cm in height and 11kg in weight.

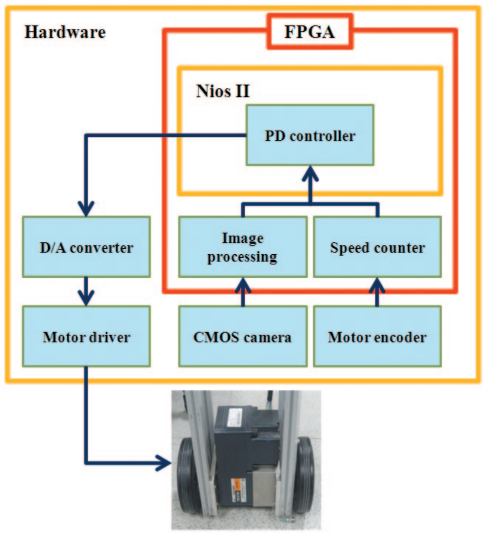

Figure 6. System architecture of the unicycle

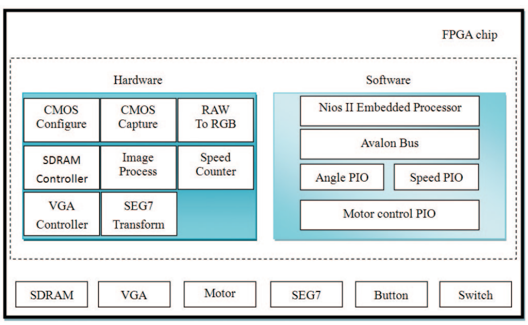

Figure 7. Software and hardware partition of the FPGA

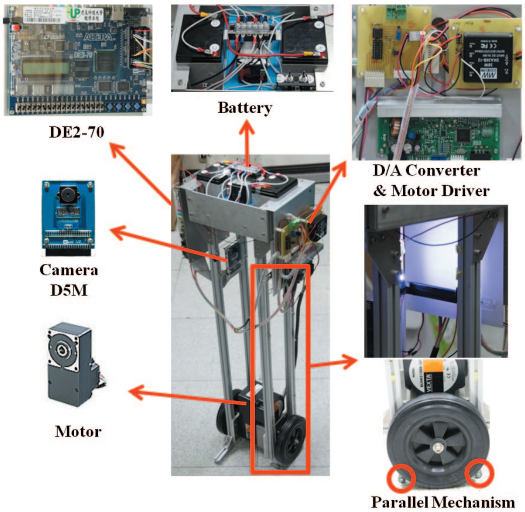

Figure 8. The resulting unicycle

VI. IMAGE PROCESSING

The CMOS camera captures the image of a white horizontal bar for computing the inclination of the unicycle, as can be seen in Figure 9. Images captured versus motions of the unicycle are demonstrated in Figure 10 and the image processing procedure is summarized in Figure 11 and explained as follows.

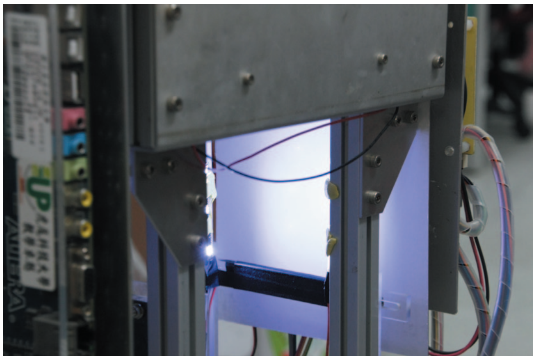

Figure 9. CMOS camera on the top of the unicycle

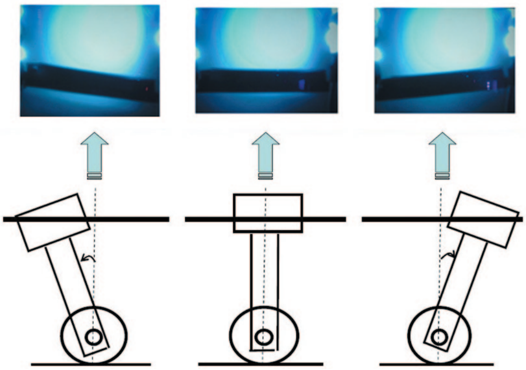

Figure 10. Images captured versus motions of the unicycle

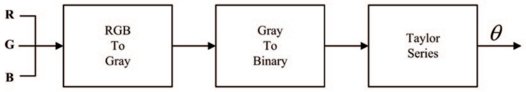

Figure 11. Image processing flow

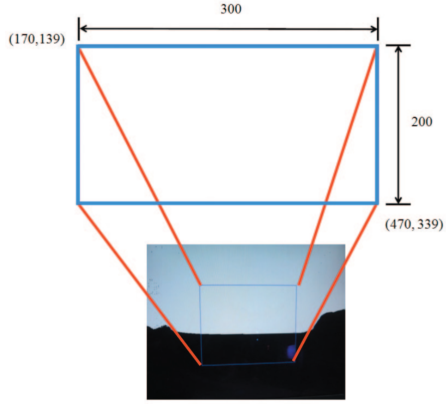

Figure 12. The image with a line in the frame

A. RGB to Gray

Add R, G, and B values of each pixel in the image and average the sum to be the resulting gray value of each pixel.

B. Gray to Binary

The purpose of this step is to filter out the noise of the image. A threshold between 0 and 255 is chosen to determine if a pixel is categorized as

1, when the pixel's gray value is greater than the threshold; as 0, vice versa.

$$\text{Binary}(x,y)=\begin{cases}1 & \text{Gray}(x,y)\geq \text{threshold}\\ 0 & \text{otherwise}\end{cases} \qquad (14)$$

C. Body Angle Computation

Draw a 640x480 rectangular frame in the binarized image which has coordinates (0, 0) on the upper left corner and (639, 479) on the lower right corner of the frame. As depicted in Figure 12, the reference line lies in the frame of the image. The vertical pixel distance b and horizontal pixel distance a are employed to calculate the angle θ according to equation (15). Since the implementation of the computation is by hardware circuit, Taylor series has been used in the circuit to approximate $\tan^{-1}(b/a)$.

$$\tan^{-1}\left(\frac{b}{a}\right)=\left(\frac{b}{a}\right)-\frac{\left(\frac{b}{a}\right)^3}{3}+\frac{\left(\frac{b}{a}\right)^5}{5}-\frac{\left(\frac{b}{a}\right)^7}{7}+\cdots \qquad (15)$$

VII. EXPERIMENTS

Double-PD control has been employed to balance the unicycle and the experimental results are exhibited in Figure 13-15 which including angle of the body, displacement of the unicycle, and control voltage, respectively. The gains are $K_{p\theta}=137$, $K_{d\theta}=60$, $K_{p\phi}=1.3$, and $K_{d\phi}=0.06$ It can be seen in 60 seconds of experimental time that the unicycle has been well controlled in accordance with the facts that the angle and displacement have been limited within ±3° and ±0.2m, respectively and the control voltage has never exceeded the limitation ±5V.

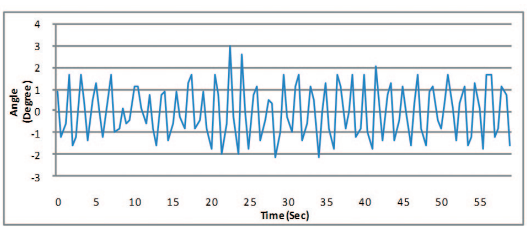

Figure 13. Double-PD experimental result (angle of the body)

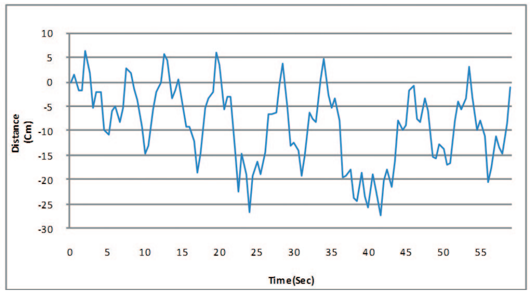

Figure 14. Double-PD experimental result (displacement of the unicycle)

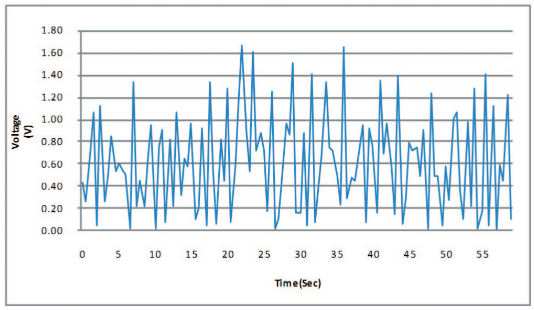

Figure 15. Double-PD experimental result (control voltage)

TABLE III. RESOURCES USAGE OF THE FPGA

<table>
<tr><td colspan="7">FPGA (70,000LEs)</td></tr>
<tr><td colspan="3">System</td><td>LEs</td><td>Total (LEs)</td><td>Hardware (LEs)</td><td>Resources usage</td></tr>
<tr><td rowspan="6">Hardware</td><td rowspan="4">Image Processing</td><td>RGB to Gray</td><td>93</td><td rowspan="4">632</td><td rowspan="6">2766</td><td rowspan="4">0.9%</td></tr>
<tr><td>Binarization</td><td>60</td></tr>
<tr><td>Coordination</td><td>33</td></tr>
<tr><td>Taylor Expansion</td><td>446</td></tr>
<tr><td colspan="2">Encoder Counter</td><td colspan="2">31</td><td>0.04%</td></tr>
<tr><td colspan="2">Other</td><td colspan="2">2103</td><td>3%</td></tr>
<tr><td colspan="3">Software</td><td colspan="3">3238</td><td>4.6%</td></tr>
<tr><td colspan="6">Total Resources usage</td><td>8.6%</td></tr>
</table>

CONCLUSIONS AND FUTURE PERSPECTIVE

This article reports the design and implementation of an electric unicycle balanced by a SoPC using the double-PD control method based on image data which is captured by a CMOS camera. From both simulation and experimental results the resulting system has met the control requirement.

The resources usage of the FPGA is summarized in Table 3. To complete the entire unicycle system it is surprising that the system has merely taken 8.6% of the FPGA resources and the speed of the image processing unit has been up to 60 images per second. According to the test results, it has been confirmed that the system outputs control commands in the speed of 5 commands per second is good enough for controlling a plant like the unicycle as we implemented.

There are still rooms for improvement this work. Firstly, next step we are going to test the control effect by applying other control methods, like back-stepping, sliding mode, and adaptive nonlinear control, to the implemented unicycle. Secondly, in the future we hope to enhance the unicycle with more functions, such as remote control, up and down slopes, carrying objects, and so on.

REFERENCES

[1]. RYNO Motors. http://rynomotors2.wordpress.com/

[2]. Segway. http://www.segway.com/

[3]. BPG Motors. http://bpg-motors.com/

[4]. X. G. Ruan, J. M. Hu, and Q. Y. Wang, "Modeling with Euler-Lagrang Equation and Cybernetical Analysis for a Unicycle Robot," Second International Conference on Intelligent Computation Technology and Automation, 2009

[5]. Z. Y. Jin, Q. Z. Zhang, "The Nonholonomic Motion Planning and Control of the Unicycle Mobile Robot," in Proceedings of the 6th World Congress on Intelligent Control and Automation, Dalian, China, June 2006

[6]. Jia-Son Lee, "Wheeled Inverted Pendulum Balancing PID Control," Department of Electric Engineering, National Taiwan University on Science and Technology, Master thesis, 2005 (in Chinese)

[7]. Yi-Long Chen, "Simulation and Applications of Real-Time Hardware in the Loop Based on the xPC Target System," Department of Engineering Science, National Cheng Kung University, Master thesis, 2010 (in Chinese)

[8]. C. N. Huang, "The Development of Selfbalancing Controller for One-Wheeled Vehicles," Engineering, 2:212–219, 2010

[9]. C. C. Tsai, S. C. Shih, and S. C. Lin "Adaptive Nonlinear Control Using RBFNN for an Electric Unicycle," in Proceedings of the IEEE International conference on System, Man and Cybernetics, Singapore, October 2008

[10]. Yuan-Pao Hsu, Hsiao-Chun Miao, Sheng-Han Huang, "A SoPC-Based Surveillance System," T.H.S. Li et al. (Eds.): FIRA 2011, CCIS 212, pp. 86-93, Kaohsiung, Taiwan, August 2011

[11]. TRDB D5M User Guide http://www.terasic.com.tw/cgi-bin/page/archive.pl?Laguage=Taiwan&CategoryNo=85&No=282&PartNo=3

[12]. Brushless Motor Systems BLH Series

[13]. http://www.orientalmotor.com/products/CatalogPdfs.htm